

# Spectral and Energy Efficiency of Cell-Free Massive MIMO Systems with Hardware Impairments

Jiayi Zhang, Yinghua Wei, Emil Björnson, Yu Han, and Xu Li

## Abstract

Cell-free massive multiple-input multiple-output (MIMO), with a large number of distributed access points (APs) that jointly serve the user equipments (UEs), is a promising network architecture for future wireless communications. To reduce the cost and power consumption of such systems, it is important to utilize low-quality transceiver hardware at the APs. However, the impact of hardware impairments on cell-free massive MIMO has thus far not been studied. In this paper, we take a first look at this important topic by utilizing well-established models of hardware distortion and deriving new closed-form expressions for the spectral and energy efficiency. These expressions provide important insights into the practical impact of hardware impairments and also how to efficiently deploy cell-free systems. Furthermore, a novel hardware-quality scaling law is presented. It proves that the impact of hardware impairments at the APs vanish as the number of APs grows. Numerical results validate that cell-free massive MIMO systems are inherently resilient to hardware impairments.

## I. INTRODUCTION

Massive MIMO is a cellular technology that equips each cell with a large number of antennas to spatially multiplex many UEs on the same time-frequency resource. It is a key technology for the fifth generation (5G) cellular networks [1]–[3], since it can offer high spectral and energy

This work was supported in part by the National Natural Science Foundation of China (Grant No. 61601020) and the Fundamental Research Funds for the Central Universities (Grant Nos. 2016RC013, 2017JBM319, and 2016JBZ003). The work of E. Björnson was supported by ELLIIT and SSF, Y. Han was supported in part by the National Science Foundation (NSFC) for Distinguished Young Scholars of China with Grant 61625106.

J. Zhang, Y. Wei, and X. Li are with the School of Electronic and Information Engineering, Beijing Jiaotong University, Beijing 100044, P. R. China (e-mail: jiayizhang@bjtu.edu.cn).

E. Björnson is with the Department of Electrical Engineering (ISY), Linköping University, Linköping, Sweden.

Y. Han is with the National Mobile Communications Research Laboratory, Southeast University, Nanjing 210096, P. R. China.

efficiency under practical conditions, which is necessary to keep up with the tremendous growing demand for wireless communications [4]. There are two topologies for cellular massive MIMO deployment: a co-located antenna array in the cell center or multiple geographically distributed antenna arrays [5]. Both topologies rely on having cells that each serves an exclusive set of UEs.

Instead of relying on cells, a network MIMO approach can be taken where geographically distributed APs are jointly serving all the UEs [6]. Cell-free massive MIMO is the latest form of network MIMO, where a massive number of single-antenna APs are deployed to phase-coherently and simultaneously serve a much smaller number of UEs, distributed over a wide area. To make the network operation scalable, a time-division duplex (TDD) protocol is used, where each AP only utilizes locally estimated channels and only data signals are distributed over the backhaul [7]. What makes cell-free massive MIMO different from classic network MIMO is the analytical approach, borrowed from cellular massive MIMO, which enables ergodic capacity analysis and efficient power control. In [8], the authors developed a max-min power control algorithm combined with linear zero-forcing precoders for cell-free massive MIMO. In [9], [10], it was indicated that cell-free massive MIMO can give a 5–10 fold gain in throughput over uncoordinated small cell systems, taking the effects of imperfect channel state information (CSI), pilot assignment and power control into consideration. In [11], the authors presented an asymptotic approximation of the signal-to-interference-plus-noise ratio (SINR) of the minimum mean-square error (MMSE) receiver. In [12], [13], the authors developed a novel low-complexity power control technique with zero-forcing precoding to maximize the energy efficiency (EE) of cell-free massive MIMO.

The aforementioned works on cell-free massive MIMO assume that the transceiver hardware of the APs is perfect. Considering that the energy consumption and deployment cost increase rapidly with the number of APs, cell-free massive MIMO systems preferably use low-cost components, which are prone to hardware impairments. It has been proved that the detrimental impact of hardware impairments at the APs of co-located massive MIMO systems vanishes asymptotically as the number of antennas grows large [5], [14]–[17], while the impairments at the UEs remain [17], [18]. Whether these properties carry over to cell-free massive MIMO systems is a practically important open question that we will answer.

In this paper, we quantitatively investigate the uplink performance of a cell-free massive MIMO with hardware impairments at APs and UEs. The main contributions are:

- We derive a closed-form expression for the uplink spectral efficiency (SE) of cell-free

massive MIMO systems with transceiver hardware impairments. This expression explicitly reveals how hardware impairments at the UEs and APs affect the SE.

- We obtain a useful hardware-quality scaling law, which establishes a precise relationship between the number of APs and the hardware quality factors. We prove that the impact of the AP hardware quality vanishes as the number of APs grows large.
- A closed-form EE expression is derived to show the optimal number of APs for different hardware qualities.

## II. SYSTEM MODEL

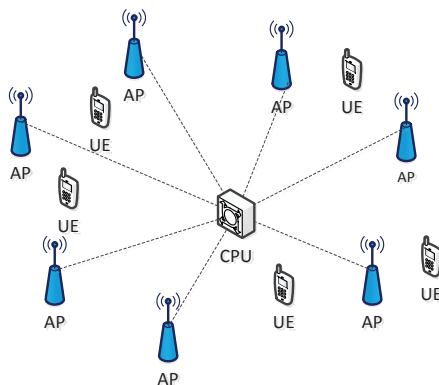


Fig. 1. Illustration of a cell-free massive MIMO system.

We consider a cell-free massive MIMO system with  $M$  APs and  $K$  UEs that are served on the same time-frequency resource. All APs and UEs are equipped with a single antenna in this paper, and they are distributed over a wide area. The APs connect to a central processing unit (CPU) via backhaul links; see Fig 1 for an illustration. We consider the classic block fading model [10], [19], where each coherence interval consists of three phases: uplink training, uplink data transmission, and downlink data transmission. In the uplink training, the UEs send pilot sequences and each AP estimates its channel to each UE. The obtained channel estimates are later used to detect the signals transmitted from the UEs in the uplink. In this paper, we only consider the uplink.

The channel coefficient  $g_{mk}$  between AP  $m$  and UE  $k$  is

$$g_{mk} \sim \mathcal{CN}(0, \beta_{mk}) \quad (1)$$

for  $m = 1, \dots, M$ ,  $k = 1, \dots, K$ . The variance  $\beta_{mk} = \mathbb{E}\{|g_{mk}|^2\}$  denotes the large-scale fading (including path loss and shadowing) and the random distribution models the Rayleigh small-scale fading.

In the uplink data transmission, the  $k$ th UE first multiplies its information symbol  $q_k \sim \mathcal{CN}(0, 1)$  by a power control coefficient  $\sqrt{\gamma_k}$ , ( $0 \leq \gamma_k \leq 1$ ). Then, all UEs simultaneously transmit their data to the APs. In prior works, the received signal at the  $m$ th AP has been given as

$$y_{um} = \sum_{k=1}^K g_{mk} \sqrt{\rho_u \gamma_k} q_k + w_{um}, \quad (2)$$

where  $\rho_u$  denotes the maximum transmit power of a UE and  $w_{um} \sim \mathcal{CN}(0, \sigma^2)$  is the additive white Gaussian noise (AWGN). This model implicitly assumes perfect transceiver hardware. In practice, the transceiver hardware of the APs and UEs suffer from hardware impairments, which distort the transmitted and received signals. To analyze the joint impact of all kinds of hardware distortion on the communication performance, we use the well-established model from [18], which is based on measurements [20]. The main characteristic of this model is that the signal power is reduced by a factor  $\kappa$  and then additive noise is added with a power that corresponds to the removed signal power. Applying this model to (2), the received signal at the  $m$ th AP is instead given by

$$y_{um} = \sum_{k=1}^K \sqrt{\kappa_r} g_{mk} (\sqrt{\rho_u \gamma_k \kappa_t} q_k + \eta_{kt}) + \eta_{mr} + w_{um}, \quad (3)$$

where  $\kappa_t$  and  $\kappa_r$  are the hardware quality factors of the transmitter and receiver, respectively. These are parameters between 0 and 1, where  $\kappa_t = \kappa_r = 1$  is perfect hardware and  $\kappa_t = \kappa_r = 0$  is useless hardware that turns everything into distortion. Measurements (e.g., [20]) have suggested that

$$\eta_{kt} \sim \mathcal{CN}(0, (1 - \kappa_t) \rho_u \gamma_k), \quad (4)$$

$$\eta_{mr} | \{g_{mk}\} \sim \mathcal{CN}\left(0, (1 - \kappa_r) \rho_u \sum_{k=1}^K \gamma_k |g_{mk}|^2\right), \quad (5)$$

where (5) is the conditional distribution given the set of channel realizations  $\{g_{mk}\}$  in a coherence interval.

The channel estimation at the APs is based on uplink pilots from the UEs. In the uplink

training phase, let  $\tau$  and  $\rho_p$  denote the pilot length and the transmit power of each pilot symbol, respectively. The  $k$ th UE sends its pilot sequences  $\sqrt{\tau}\boldsymbol{\varphi}_k \in \mathbb{C}^{\tau \times 1}$ , which satisfies  $\|\boldsymbol{\varphi}_k\|^2 = 1$ . Based on the system model (3), the received pilot vector  $\mathbf{y}_{pm} \in \mathbb{C}^{\tau \times 1}$  at the  $m$ th AP is

$$\mathbf{y}_{pm} = \sum_{k=1}^K \sqrt{\kappa_r} g_{mk} \left( \sqrt{\tau \rho_p \kappa_t} \boldsymbol{\varphi}_k + \boldsymbol{\eta}_{kt} \right) + \boldsymbol{\eta}_{mr} + \mathbf{w}_{pm}, \quad (6)$$

where  $\mathbf{w}_{pm} \sim \mathcal{CN}(\mathbf{0}, \sigma^2 \mathbf{I}_\tau)$  is a vector of AWGN. Assuming that the distortion is independent between samples in the coherence interval, the transmitter distortion vector is  $\boldsymbol{\eta}_{kt} \sim \mathcal{CN}(\mathbf{0}, \rho_p (1 - \kappa_t) \mathbf{I}_\tau)$  and the receiver distortion vector is  $\boldsymbol{\eta}_{mr} \{g_{mk}\} \sim \mathcal{CN}(\mathbf{0}, \rho_p (1 - \kappa_r) \sum_{k=1}^K |g_{mk}|^2 \mathbf{I}_\tau)$ .

Having completed the pilot transmission, the first step towards estimating the channel  $g_{mk}$  from UE  $k$  is to perform a despreading operation [19]. More precisely, the AP takes the inner product between  $\boldsymbol{\varphi}_k$  and  $\mathbf{y}_{pm}$  to obtain  $\tilde{y}_{p,mk} = \boldsymbol{\varphi}_k^H \mathbf{y}_{pm}$ . The linear MMSE (LMMSE) estimate of  $g_{mk}$  based on  $\tilde{y}_{p,mk}$  is then given by

$$\hat{g}_{mk} = \frac{\mathbb{E}\{\tilde{y}_{p,mk}^* g_{mk}\}}{\mathbb{E}\left\{\left|\tilde{y}_{p,mk}\right|^2\right\}} \tilde{y}_{p,mk} = c_{mk} \tilde{y}_{p,mk}, \quad (7)$$

where  $c_{mk}$  is given in

$$c_{mk} \triangleq \frac{\sqrt{\tau \rho_p \kappa_r \kappa_t} \beta_{mk}}{\rho_p \sum_{k'=1}^K \beta_{mk'} \left( \kappa_r \kappa_t \tau |\boldsymbol{\varphi}_k^H \boldsymbol{\varphi}_{k'}|^2 + (1 - \kappa_r \kappa_t) \right) + \sigma^2} \quad (8)$$

and

$$\lambda_{mk} \triangleq \mathbb{E}\left\{|\hat{g}_{mk}|^2\right\} = \sqrt{\tau \rho_p \kappa_r \kappa_t} \beta_{mk} c_{mk}. \quad (9)$$

During uplink data transmission, the  $m$ th AP multiplies its received signal  $y_{um}$  in (3) with the conjugate of the LMMSE estimate  $\hat{g}_{mk}$ . Then, each AP sends its obtained quantity  $\hat{g}_{mk}^* y_{um}$  to the CPU via the backhaul. The combined received signal at the CPU is the maximum ratio combined scalar

$$r_{uk} = \sum_{m=1}^M \hat{g}_{mk}^* y_{um}. \quad (10)$$

### III. PERFORMANCE ANALYSIS

The received signal in (10) can be expanded as

$$\begin{aligned}
r_{uk} = & \underbrace{\sqrt{\rho_u \gamma_k \kappa_r \kappa_t} Q_k \sum_{m=1}^M \hat{g}_{mk}^* g_{mk}}_{k\text{th UE's signal}} + \underbrace{\sum_{m=1}^M \hat{g}_{mk}^* w_{um}}_{\text{compound noise}} \\
& + \underbrace{\sqrt{\rho_u \kappa_r \kappa_t} \sum_{m=1}^M \sum_{k' \neq k}^K \sqrt{\gamma_{k'}} Q_{k'} \hat{g}_{mk'}^* g_{mk'}}_{\text{inter-UE interference}} \\
& + \underbrace{\sum_{m=1}^M \sum_{k'=1}^K \sqrt{\kappa_r} \hat{g}_{mk'}^* g_{mk'} \eta_{k't} + \sum_{m=1}^M \hat{g}_{mk}^* \eta_{mr}}_{\text{hardware impairments}}. \tag{11}
\end{aligned}$$

It is clear that  $r_{uk}$  consists of four parts: the desired signal from the  $k$ th UE, the compound noise, the inter-UE interference, and the distortion caused by hardware impairments in the UEs' and APs' hardware. It is the last term that makes the analysis in this paper different from prior works, which have assumed perfect hardware. In this section, we will use (11) to characterize the SE and EE.

#### A. Spectral Efficiency

We begin by deriving a closed-form expression for an uplink SE, which is a lower bound on the ergodic capacity. Since the estimate and estimation error are non-Gaussian distributed due to the hardware impairments, we cannot use the standard capacity lower bound from [2]. The following closed-form SE expression is instead derived using the use-and-then-forget capacity bounding technique [19].

**Theorem 1.** *In cell-free massive MIMO with hardware impairments, the uplink capacity of the  $k$ th UE is lower bounded by*

$$R_{uk} = \log_2 \left( 1 + \frac{\kappa_r \kappa_t A}{\kappa_r B + \kappa_r C - \kappa_r \kappa_t A + (1 - \kappa_r) D + E} \right), \tag{12}$$

where

$$A \triangleq \gamma_k \left( \sum_{m=1}^M \lambda_{mk} \right)^2,$$

$$B \triangleq \sum_{k'=1}^K \gamma_{k'} \left( \sum_{m=1}^M \lambda_{mk} \beta_{mk'} + \rho_p (1 - \kappa_r) \sum_{m=1}^M c_{mk}^2 \beta_{mk'}^2 \right),$$

$$C \triangleq \sum_{k'=1}^K \gamma_{k'} \left( |\varphi_k^H \varphi_{k'}|^2 + \frac{1 - \kappa_t}{\kappa_t \tau} \right) \left( \sum_{m=1}^M \lambda_{mk} \frac{\beta_{mk'}}{\beta_{mk}} \right)^2,$$

$$D \triangleq \sum_{m=1}^M \left( \lambda_{mk} \sum_{k'=1}^K \gamma_{k'} \beta_{mk'} + c_{mk}^2 (1 - \kappa_r) \rho_p \beta_{mk}^2 \right. \\ \left. + c_{mk}^2 \kappa_r \rho_p \beta_{mk'} \left( \tau \kappa_t |\varphi_k^H \varphi_{k'}|^2 + (1 - \kappa_t) \right) \right),$$

$$E \triangleq \frac{\sigma^2}{\rho_u} \sum_{m=1}^M \lambda_{mk}.$$

*Proof:* Please refer to Appendix. ■

Theorem 1 reveals that the SE increases with the number of APs, which happens when more APs are deployed. The terms  $B$  and  $C$  in the denominator represents the power of the non-coherent and coherent signals, respectively, from which the desired part  $A$  is subtracted. The remainder is interference and the coherent part is due to pilot contamination, caused by pilot reuse and the break of pilot orthogonality by the distortion. The terms  $D$  and  $E$  represent distortion in the receiving AP and additive noise, respectively. We notice that the SE increases with  $\rho_u$ , since it increases the SNR. What is less obvious is that the SE increases with the hardware quality terms  $\kappa_t$  and  $\kappa_r$ , but this will be shown numerically in Section IV.

We will now study the SE behavior when we add APs. We assume that the APs are arbitrarily distributed within a finite-sized area, such that  $\beta_{\min} \leq \beta_{mk} \leq \beta_{\max}$  for all  $m$ , where  $0 < \beta_{\min}$ ,  $\beta_{\max} < \infty$ . We then have the following result.

**Corollary 1.** *Suppose the hardware quality factors are replaced by  $\kappa_t = \frac{\kappa_{t0}}{M^{z_t}}$ ,  $\kappa_r = \frac{\kappa_{r0}}{M^{z_r}}$ , for some constant  $\kappa_{t0}, \kappa_{r0} > 0$ , where  $z_t, z_r$  denote scaling exponents in transmitters and receivers, respectively. If  $z_t > 0$  and  $z_r \geq 0$  (or  $z_t = 0$  and  $z_r > 1/2$ ), then*

$$R_{uk} \rightarrow 0, \quad \text{as } M \rightarrow \infty. \quad (13)$$

If instead  $z_t = 0$  and  $0 < z_r < 1/2$ , then  $R_{uk} \rightarrow \log_2(1 + \text{SIR}_k^\infty)$  as  $M \rightarrow \infty$ , where

$$\text{SIR}_k^\infty = \frac{\kappa_{t0}}{\sum_{k'=1}^K \frac{\gamma_{k'}}{\gamma_k} \left( |\boldsymbol{\varphi}_k^H \boldsymbol{\varphi}_{k'}|^2 + \frac{1-\kappa_{t0}}{\kappa_{t0}\tau} \right) \frac{\left( \sum_{m=1}^M \mu_{mk} \frac{\beta_{mk'}}{\beta_{mk}} \right)^2} \left( \sum_m \mu_{mk} \right)^2} - \kappa_{t0} \quad (14)$$

and  $\mu_{mk} = \frac{\rho_p \beta_{mk}^2}{\rho_p \beta_{mk} + \sigma^2}$ .

*Proof:* We divide all terms in (12) by  $\kappa_r \kappa_t A$  to obtain

$$R_{uk} = \log_2 \left( 1 + \frac{1}{\frac{B}{\kappa_t A} + \frac{C}{\kappa_t A} - 1 + \frac{(1-\kappa_r)D}{\kappa_r \kappa_t A} + \frac{E}{\kappa_r \kappa_t A}} \right).$$

Under the assumption that all  $\beta_{mk}$  are strictly non-zero and bounded, it is straightforward to show that  $\frac{C}{\kappa_t A} - 1 = \mathcal{O}(M^{2z_t})$ , which implies that  $R_{uk} \rightarrow 0$  unless  $z_t = 0$ . We further notice that  $\frac{B}{\kappa_t A} + \frac{(1-\kappa_r)D}{\kappa_r \kappa_t A} + \frac{E}{\kappa_r \kappa_t A} = \mathcal{O}(M^{2z_r-1})$  when  $z_t = 0$  and  $z_r \geq 0$ , thus these terms vanish asymptotically if  $2z_r - 1 < 0$  or  $z_r < 1/2$ . In contrast, if  $z_r > 1/2$ , these terms grow unboundedly and  $R_{uk} \rightarrow 0$ . This proves (13).

In the case of  $z_t = 0$  and  $0 < z_r < 1/2$ , all term in the denominator vanishes, except “-1” and

$$\frac{C}{\kappa_t A} \rightarrow \frac{\sum_{k'=1}^K \gamma_{k'} \left( |\boldsymbol{\varphi}_k^H \boldsymbol{\varphi}_{k'}|^2 + \frac{1-\kappa_{0t}}{\kappa_{0t}\tau} \right) \left( \sum_{m=1}^M \mu_{mk} \frac{\beta_{mk'}}{\beta_{mk}} \right)^2}{\kappa_{0t} \gamma_k \left( \sum_m \mu_{mk} \right)^2}.$$

This leads to the asymptotic expression in (14). ■

Corollary 1 proves that the APs can tolerate much lower hardware quality as the number of APs increases. However, the hardware quality of the UEs cannot be reduced without suffering a substantial performance loss. This is an important result for practical deployment of cell-free massive MIMO systems, since it indicates that low-cost AP hardware can be used. Note that a similar result has been shown for cellular massive MIMO in [5], [18], but for co-located arrays with many antennas, which is a very different topology.

## B. Energy Efficiency

In the following, we consider the EE of cell-free massive MIMO systems to see how it is affected by the number of APs. The EE (bit/Joule) is defined as the ratio of the sum rate (bit/s)



to the total power consumption (Watt) of the system. As in [13], we consider a realistic power consumption model where the total power consumption includes the power consumption of the transmitters, receivers, and backhaul. More precisely, the total power consumption is modeled as

$$P_{\text{total}} = \sum_{k=1}^K P_k + \sum_{m=1}^M P_m + \sum_{m=1}^M P_{b,m}, \quad (15)$$

where  $P_m$  denotes the circuit power consumption at the  $m$ th AP (including analog transceiver components and digital signal processing),  $P_{b,m}$  is the power consumed by the backhaul link connecting CPU and the  $m$ th AP, and  $P_k$  is the power consumption at the  $k$ th UE (including the radiated transmission power, amplifier inefficiency and the circuit power). Then, the EE can be expressed as

$$\text{EE} = \sum_{k=1}^K R_{uk} \cdot B \left/ \left( \sum_{k=1}^K P_k + \sum_{m=1}^M P_m + \sum_{m=1}^M P_{b,m} \right) \right., \quad (16)$$

where  $B$  denotes the bandwidth.

#### IV. NUMERICAL RESULTS

In this section, we study the SE and EE numerically. We assume that the  $M$  APs and  $K$  UEs are independently and uniformly distributed within a square of size  $1 \times 1$  km<sup>2</sup>. The variance  $\beta_{mk}$  in (1) is computed as

$$\beta_{mk} = L_{mk}^{-\alpha} \cdot 10^{\frac{z_{mk}}{10}}, \quad (17)$$

where  $L_{mk}$  (km) is the distance between the  $k$ th UE and  $m$ th AP,  $\alpha$  is the path loss exponent, and  $z_{mk} \sim \mathcal{N}(0, \sigma_{sh}^2)$  is the shadow fading. We also use the simulation parameters summarized in Table I. The noise variance is computed as  $\sigma^2 = B \cdot k_B \cdot T_0 \cdot \text{noise figure}$  (W), where  $k_B = 1.381 \cdot 10^{-23}$  (Joule per Kelvin), and  $T_0 = 290$  (Kelvin).

The Monte Carlo simulated and analytical average SE in (12) are compared in Fig. 2, as a function of the number of APs. It is clear to see that the analytical and simulated curves are almost the same for all considered cases. The average SE is an increasing function of  $M$ . The SE decreases when the hardware qualities  $\kappa_t$  and  $\kappa_r$  decrease. Nevertheless, Fig. 2 shows that the SE is mainly limited by the hardware impairments at the UE (e.g.,  $\kappa_t = 0.98$  gives a larger impact than  $\kappa_r = 0.98$ ).

TABLE I  
KEY SIMULATION PARAMETERS

Parameters	Values
noise figure	9 dB
$B$	20 MHz
$\rho_p, \rho_u$	100 mW
$\sigma_{sh}$	8 dB
$\alpha$	3.5
$\gamma_k$	1

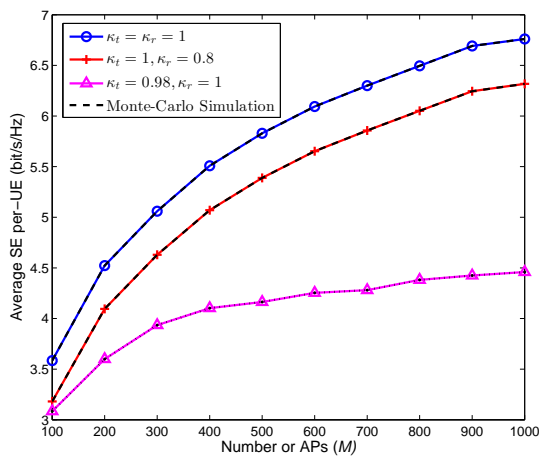


Fig. 2. Average SE per-UE as a function of the number of APs for  $K = 10$ . Here,  $\tau = K$  and all pilot sequences are pairwise orthogonal.

Fig. 3 validates the hardware-quality scaling law established by Corollary 1. When  $z_t = z_r = 0$ , the SE increases with  $M$  without bound. When  $z_t = 0, 0 \leq z_r < 1/2$  (e.g.,  $z_r = 0.4$ ), we observe that the SE converges to a non-zero limit. Moreover, the SE converges to zero when  $z_r = 0, z_t > 0$ .

Fig. 4 presents the CDF of the per-UE SE with  $M = 200, K = 60$ , and  $\tau = 20$ , for different hardware qualities  $\kappa_t$  and  $\kappa_r$ . We find that around 80% of the SE values are distributed between 1.96 and 2.2 for  $\kappa_t = \kappa_r = 1$ , while the range is 1.89 – 2.1 for  $\kappa_t = \kappa_r = 0.98$  and 1.8 – 1.92 for  $\kappa_t = \kappa_r = 0.95$ . Hence, the uplink per-UE SE for  $\kappa_t = \kappa_r = 1$  is only 5% higher than in the case when  $\kappa_t = \kappa_r = 0.95$ .

Fig. 5 investigates the EE in (16) as a function of the number of APs for different values of  $P_m$ . We consider  $K = 20, P_k = 0.6$  W, and  $P_{b,m} = 0.1$  W. We observe that the EE decreases when increasing  $P_m$ , for the same number of APs, due to the larger power consumption. There is a value  $M^{\text{opt}}$  that provides maximum EE. For  $P_m = 0.0125$ , this value is  $M^{\text{opt}} = 40$ . When

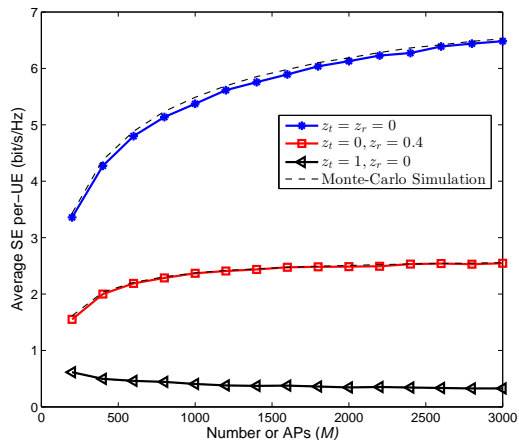


Fig. 3. Average SE per-UE against the number of APs for different hardware scaling factors  $z_t$ ,  $z_r$ .

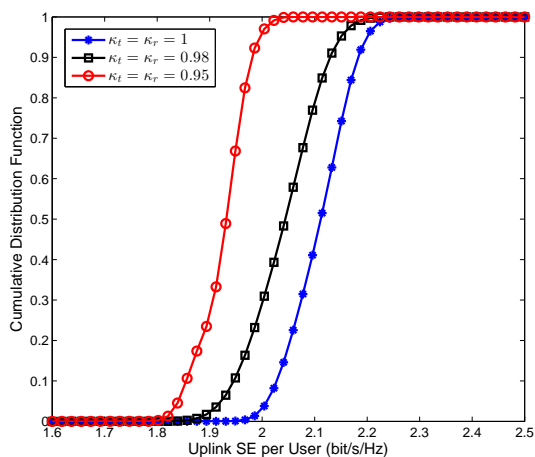


Fig. 4. SE CDF for different levels of hardware impairments  $\kappa_t$  and  $\kappa_r$  ( $M = 200$ ,  $K = 60$ ).

$M \leq M^{\text{opt}}$ , the EE can be improved by increasing  $M$ . However, when  $M > M^{\text{opt}}$ , increasing  $M$  will rapidly reduce the EE. This is due to the fact that only a few APs have a large impact on the SE of a UE, thus adding more APs will increase the power consumption linearly, while the sum SE might increase more slowly.

## V. CONCLUSION

This paper has taken a first look at the impact of transceiver hardware impairments on the performance of cell-free massive MIMO systems, using a well-established distortion model. Closed-form expressions for the SE and EE were obtained, which reveal how the performance depends on the hardware quality factors of the APs and UEs, the number of APs  $M$ , and the number of UEs  $K$ . Furthermore, a hardware-quality scaling law was established. It proves that

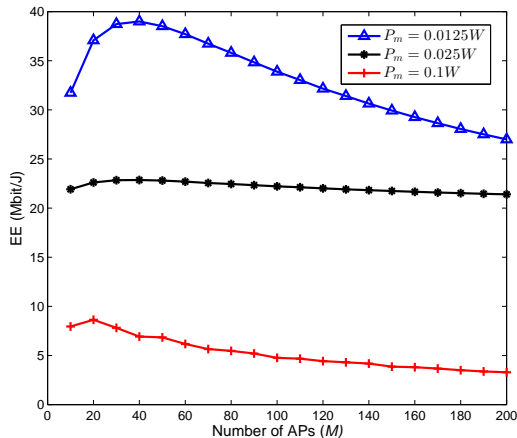


Fig. 5. EE as a function of the number of APs for different power consumption  $P_m$  ( $K = 20$ ,  $P_k = 0.6$  W, and  $P_{b,m} = 0.1$  W).

the detrimental effect of hardware impairments at the APs vanishes when the number of APs grows large (in a finite-sized deployment area), while the effect of hardware impairments at the UEs remain. This indicates that cell-free massive MIMO can be deployed using low-quality hardware. In future work, more detailed and specialized hardware impairment models can be used to validate these observations.

## VI. APPENDIX

The received signal  $r_{uk}$  in (11) can be rewritten as

$$\begin{aligned}
 r_{uk} = & \text{DS}_k \cdot q_k + \text{BU}_k \cdot q_k + \sum_{k' \neq k}^K \text{UI}_{kk'} \cdot q_{k'} \\
 & + \sum_{k'=1}^K \text{HI}_{tkk'}^{\text{UE}} + \text{HI}_r^{\text{AP}} + \text{NI}_k,
 \end{aligned} \tag{18}$$

where

$$\begin{aligned}
 \text{DS}_k & \triangleq \sqrt{\rho_u \gamma_k \kappa_r \kappa_t} \mathbb{E} \left\{ \sum_{m=1}^M \hat{g}_{mk}^* g_{mk} \right\}, \\
 \text{BU}_k & \triangleq \sqrt{\rho_u \gamma_k \kappa_r \kappa_t} \left( \sum_{m=1}^M \hat{g}_{mk}^* g_{mk} - \mathbb{E} \left\{ \sum_{m=1}^M \hat{g}_{mk}^* g_{mk} \right\} \right), \\
 \text{UI}_{kk'} & \triangleq \sqrt{\rho_u \kappa_r \kappa_t \gamma_{k'}} \sum_{m=1}^M \hat{g}_{mk}^* g_{mk'},
 \end{aligned}$$

$$\mathbf{HI}_{tkk'}^{\text{UE}} \triangleq \sum_{m=1}^M \sqrt{\kappa_r} \hat{g}_{mk}^* g_{mk'} \eta_{k't},$$

$$\mathbf{HI}_r^{\text{AP}} \triangleq \sum_{m=1}^M \hat{g}_{mk}^* \eta_{mr}, \quad \mathbf{NI}_k \triangleq \sum_{m=1}^M \hat{g}_{mk}^* w_{um}.$$

By using the use-and-then-forget bounding technique [19, Chapter 3], the achievable SE of the  $k$ th UE is obtained as

$$\mathbf{R}_{uk} = \log_2 \left( 1 + \frac{|\mathbf{DS}_k|^2}{\mathbb{E}\{|\mathbf{BU}_{kk'}|^2\} + \sum_{k' \neq k}^K \mathbb{E}\{|\mathbf{UI}_{kk'}|^2\} + \sum_{k'=1}^K \mathbb{E}\{|\mathbf{HI}_{tkk'}^{\text{UE}}|^2\} + \mathbb{E}\{|\mathbf{HI}_r^{\text{AP}}|^2\} + \mathbb{E}\{|\mathbf{NI}_k|^2\}} \right). \quad (19)$$

It is straightforward, but tedious, to compute the following expectations:

$$|\mathbf{DS}_k|^2 = \rho_u \gamma_k \kappa_r \kappa_t \left( \sum_{m=1}^M \lambda_{mk} \right)^2, \quad (20)$$

$$\begin{aligned} \mathbb{E}\{|\mathbf{BU}_k|^2\} &= \rho_u \gamma_k \kappa_r \kappa_t \left( \sum_{m=1}^M \gamma_{mk} \beta_{mk} + \frac{1 - \kappa_t}{\kappa_t \mathcal{T}} \left( \sum_{m=1}^M \lambda_{mk} \right)^2 \right. \\ &\quad \left. + \rho_p (1 - \kappa_r) \sum_{m=1}^M c_{mk}^2 \beta_{mk}^2 \right), \end{aligned} \quad (21)$$

$$\sum_{k' \neq k}^K \mathbb{E}\{|\mathbf{UI}_{kk'}|^2\} = \rho_u \kappa_r \kappa_t \sum_{k' \neq k}^K \gamma_{k'} \Omega_{kk'}, \quad (22)$$

where

$$\begin{aligned} \Omega_{kk'} &\triangleq \mathbb{E} \left\{ \left| \sum_{m=1}^M \hat{g}_{mk}^* g_{mk'} \right|^2 \right\} = \left( \sum_{m=1}^M \lambda_{mk} \beta_{mk'} \right. \\ &\quad \left. + \left( |\boldsymbol{\varphi}_k^H \boldsymbol{\varphi}_{k'}|^2 + \frac{1 - \kappa_t}{\kappa_t \mathcal{T}} \right) \left( \sum_{m=1}^M \lambda_{mk} \frac{\beta_{mk'}}{\beta_{mk}} \right)^2 \right. \\ &\quad \left. + \rho_p (1 - \kappa_r) \sum_{m=1}^M c_{mk}^2 \beta_{mk'}^2 \right). \end{aligned} \quad (23)$$

This expression is also utilized to compute

$$\sum_{k'=1}^K \mathbb{E} \left\{ \left| \mathbf{H}_{tkk'}^{\text{UE}} \right|^2 \right\} = \rho_u \kappa_r (1 - \kappa_t) \sum_{k'=1}^K \gamma_{k'} \Omega_{kk'}, \quad (24)$$

$$\begin{aligned} \mathbb{E} \left\{ \left| \mathbf{H}_r^{\text{AP}} \right|^2 \right\} &= (1 - \kappa_r) \rho_u \sum_{m=1}^M \left( \lambda_{mk} \sum_{k'=1}^K \gamma_{k'} \beta_{mk'} \right. \\ &+ c_{mk}^2 \kappa_r \rho_p \beta_{mk'} \left( \tau \kappa_t \left| \boldsymbol{\varphi}_k^H \boldsymbol{\varphi}_{k'} \right|^2 + (1 - \kappa_t) \right) \\ &\left. + c_{mk}^2 (1 - \kappa_r) \rho_p \beta_{mk'}^2 \right), \end{aligned} \quad (25)$$

$$\mathbb{E} \left\{ \left| \mathbf{N}_k \right|^2 \right\} = \sigma^2 \sum_{m=1}^M \lambda_{mk}. \quad (26)$$

The proof is completed by substituting (20)–(26) into (19).

## REFERENCES

- [1] W. Liu, S. Han, and C. Yang, “Energy efficiency scaling law of massive MIMO systems,” *IEEE Trans. Commun.*, vol. 65, no. 1, pp. 107–121, Jan. 2017.
- [2] J. Hoydis, S. ten Brink, and M. Debbah, “Massive MIMO in the UL/DL of cellular networks: How many antennas do we need?” *IEEE J. Sel. Areas Commun.*, vol. 31, no. 2, pp. 160–171, Feb. 2013.
- [3] F. Boccardi, R. W. Heath, A. Lozano, T. L. Marzetta, and P. Popovski, “Five disruptive technology directions for 5G,” *IEEE Commun. Mag.*, vol. 52, no. 2, pp. 74–80, Feb. 2014.
- [4] E. Björnson, E. G. Larsson, and T. L. Marzetta, “Massive MIMO: Ten myths and one critical question,” *IEEE Commun. Mag.*, vol. 54, no. 2, pp. 114–123, Feb. 2016.
- [5] E. Björnson, M. Matthaiou, and M. Debbah, “Massive MIMO with non-ideal arbitrary arrays: Hardware scaling laws and circuit-aware design,” *IEEE Trans. Wireless Commun.*, vol. 14, no. 8, pp. 4353–4368, Aug. 2015.
- [6] S. Venkatesan, A. Lozano, and R. Valenzuela, “Network MIMO: Overcoming intercell interference in indoor wireless systems,” in *Proc. 2007 41st Asilomar Conf. on Signals, Systems and Computers*, Nov. 2007, pp. 83–87.
- [7] E. Björnson, R. Zakhour, D. Gesbert, and B. Ottersten, “Cooperative multicell precoding: Rate region characterization and distributed strategies with instantaneous and statistical CSI,” *IEEE Trans. Signal Process.*, vol. 58, no. 8, pp. 4298–4310, Aug. 2010.
- [8] E. Nayebi, A. Ashikhmin, T. L. Marzetta, H. Yang, and B. D. Rao, “Precoding and power optimization in cell-free massive MIMO systems,” *IEEE Trans. Wireless Commun.*, vol. 16, no. 7, pp. 4445–4459, Apr. 2017.
- [9] H. Q. Ngo, A. Ashikhmin, H. Yang, E. G. Larsson, and T. L. Marzetta, “Cell-free massive MIMO: Uniformly great service for everyone,” in *Proc. IEEE Int. Workshop on Signal. Process. Adv. Wireless Commun. (SPAWC), Stockholm, Sweden*, Jun. 2015, pp. 201–205.
- [10] —, “Cell-free massive MIMO versus small cells,” *IEEE Trans. Wireless Commun.*, vol. 16, no. 3, pp. 1834–1850, Mar. 2017.

- [11] E. Nayebi, A. Ashikhmin, T. L. Marzetta, and B. D. Rao, "Performance of cell-free massive MIMO systems with MMSE and LSFD receivers," in *Proc. 50th Asilomar Conf. on Signals, Systems and Computers*. IEEE, Nov. 2016, pp. 203–207.
- [12] L. D. Nguyen, T. Q. Duong, H. Q. Ngo, and K. Tourki, "Energy efficiency in cell-free massive MIMO with zero-forcing precoding design," *IEEE Commun. Lett.*, to appear, 2017.
- [13] H. Q. Ngo, L.-N. Tran, T. Q. Duong, M. Matthaiou, and E. G. Larsson, "On the total energy efficiency of cell-free massive MIMO," *arXiv:1702.07601*, Feb. 2017.
- [14] Z. Zhang, Z. Chen, M. Shen, and B. Xia, "Spectral and energy efficiency of multipair two-way full-duplex relay systems with massive MIMO," *IEEE J. Sel. Areas Commun.*, vol. 34, no. 4, pp. 848–863, Apr. 2016.
- [15] J. Zhang, L. Dai, Z. He, S. Jin, and X. Li, "Performance analysis of mixed-ADC massive MIMO systems over Rician fading channels," *IEEE J. Sel. Areas Commun.*, vol. 35, no. 6, pp. 1327–1338, Jun. 2017.
- [16] J. Zhang, L. Dai, S. Sun, and Z. Wang, "On the spectral efficiency of massive MIMO systems with low-resolution ADCs," *IEEE Commun. Lett.*, vol. 20, no. 5, pp. 842–845, May. 2016.
- [17] J. Zhang, L. Dai, X. Zhang, E. Björnson, and Z. Wang, "Achievable rate of Rician large-scale MIMO channels with transceiver hardware impairments," *IEEE Trans. Veh. Technol.*, vol. 65, no. 10, pp. 8800–8806, Oct. 2016.
- [18] E. Björnson, J. Hoydis, M. Kountouris, and M. Debbah, "Massive MIMO systems with non-ideal hardware: Energy efficiency, estimation, and capacity limits," *IEEE Trans. Inf. Theory*, vol. 60, no. 11, pp. 7112–7139, Nov. 2014.
- [19] T. L. Marzetta, E. G. Larsson, H. Yang, and H. Q. Ngo, *Fundamentals of Massive MIMO*. Cambridge University Press, 2016.
- [20] C. Studer, M. Wenk, and A. Burg, "MIMO transmission with residual transmit-RF impairments," in *Proc. 2010 ITG/IEEE Works. Smart Ant.*, 2010, pp. 189–196.